RAPID COMMUNICATIONS

PHYSICAL REVIEW B

CONDENSED MATTER

THIRD SERIES, VOLUME 52, NUMBER 24 15 DECEMBER 1995-II

RAPID COMMUNICATIONS

Rapid Communications are intended for the accelerated publication of important new results and are therefore given priority treatment both in the editorial office and in production. A Rapid Communication in **Physical Review B** *may be no longer than four printed pages and must be accompanied by an abstract. Page proofs are sent to authors.*

Polarization and dynamical charge of ZnO within different one-particle schemes

S. Massidda
Istituto Nazionale di Fisica Moleculare, Dipartimento di Scienze Fisiche, Università degli Studi di Cagliari, I-09124 Cagliari, Italy and Institut Romand de Recherche Numérique en Physique des Matériaux (IRRMA), PHB Ecublens, CH-1015 Lausanne, Switzerland

R. Resta
Istituto Nazionale di Fisica Moleculare, Dipartimento di Fisica Teorica, Università di Trieste, I-34014 Trieste, Italy and Institut Romand de Recherche Numérique en Physique des Matériaux (IRRMA), PHB Ecublens, CH-1015 Lausanne, Switzerland

M. Posternak and A. Baldereschi
Institut Romand de Recherche Numérique en Physique des Matériaux (IRRMA), PHB Ecublens, CH-1015 Lausanne, Switzerland
(Received 11 September 1995)

We calculate *ab initio* the electronic states, spontaneous polarization P, and Born dynamical charge Z^* of ZnO, using the local-density approximation (LDA), the Hartree-Fock (HF), and a model GW scheme. Upon going from HF to GW and to LDA, the d bands raise substantially in energy, the model GW providing the best overall agreement with experiment. By contrast, the three schemes give the concordant values $P=-0.047$ C/m^2 and $Z^*=\pm 2.1$, in agreement with available experimental data. While the value of Z^* suggests a rigid-ion-like behavior of ZnO, its band-by-band decomposition reveals anomalous contributions from O $2s$, Zn $3d$, and O $2p$ bands, indicating a substantial interaction between the corresponding *occupied* atomic orbitals.

The wurtzite structure is the simplest crystal structure where spontaneous polarization is allowed by symmetry. Amongst the wurtzite crystals, ZnO is probably the most studied and important one technologically.[1] Some first-principles studies of ZnO have been published, focusing in particular on structural properties,[2–4] and based on the local-density approximation[2,4] (LDA) to density-functional theory (DFT), and Hartree-Fock[3] (HF) approximation. Both theoretical schemes have merits and shortcomings, particularly for materials having a mixed ionic/covalent character, such as ZnO. Concerning the spontaneous polarization of ZnO, we have investigated it,[4] together with its derivative with respect to sublattice displacement, i.e., the Born effective charge Z^* within DFT-LDA. Since polarization phenomena are often dominated by delicate hybridization mechanisms,[5] one wonders whether LDA provides a reliable framework for their description in the present material.

Photoemission experiments, as well as band-structure calculations, have pointed out that the zinc d electrons interact substantially with the oxygen p ones. Incidentally, this feature implies that any frozen-core or otherwise simple (sp) pseudopotential approach is unreliable. We expect that when comparing the *occupied* one-electron states of ZnO, as obtained from LDA and from HF ground-state all-electron calculations, the dominant difference is indeed in the zinc d states, and, in particular, their energy location with respect to the highest (mostly O $2p$) valence bands.

For this reason, we study here the spontaneous polarization and the effective charge of ZnO at the HF level. To our knowledge, no similar study within HF or other first-principles scheme beyond LDA is available so far, not only for ZnO, but for *any* material. Therefore, this work generalizes the implementation of the geometric-phase theory of macroscopic polarization[6] outside the DFT framework, on a test case where different schemes produce different electronic ground states. We also present results from a third one-electron scheme, the model GW of Refs. 7 and 8, which is in a sense intermediate between the LDA and the HF ones,

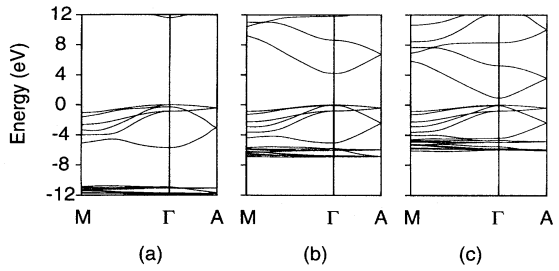

FIG. 1. Energy bands of wurtzite ZnO calculated within three different schemes: (a) Hartree-Fock, (b) model GW, and (c) local-density approximation. O $2s$ bands are located at lower energy.

and probably closer to physical reality. We anticipate that the spontaneous polarization and Born effective charge of ZnO are almost insensitive to scheme differences, and we provide a rationale for it.

All the calculations have been performed on the same footing, using the full-potential linearized-augmented-plane-wave method[9] and the same technical ingredients and experimental values of the structural parameters as in Ref. 4. Details concerning the HF implementation are given in Ref. 10. The parameters of the model GW calculation (see Ref. 8) are $\varepsilon_\infty = 3.7$ and $q_{\rm cut} = 2.5$ a.u.

The one-electron states calculated with the three schemes differ considerably. The three band structures are displayed in Fig. 1, and some related numerical data are reported in Table I. As usual, the HF gap is much larger than the experimental one, while the LDA gap is too small. Not surprisingly, the model GW provides the best value, within 0.8 eV from the experiment (Table I). In the present work we focus on ground-state properties, hence on the occupied states, whose quasiparticle removal energies have been measured in photoemission experiments. Although this is common practice, it is not quite legitimate to compare LDA or HF bands with photoemission spectra, while, on the other hand, it is appropriate in the case of GW, which aims indeed at calculating such energies. Figure 1 shows two groups of occupied bands, which can be characterized as being mostly of zinc d and of oxygen p character. They are well separated in the HF band structure, while they show increasing overlap going to GW and LDA, thus suggesting different degrees of hybridization. The p bandwidth decreases from HF to GW and to LDA, its value being predicted quite accurately by the model GW (Table I), while the d bandwidth increases from HF to GW and to LDA. As for the location of the center of the d bands (relative to the valence-band edge), the LDA value is much higher than the experimental one, and the HF much lower. Again the model GW is more successful and shows an error of about 1 eV (Table I), the origin of which is likely the neglect in the long-range Coulomb correction [Eq. (2) of Ref. 8] of dynamical screening and local-field effects *beyond* LDA. Since the latter are presumably rather important in ZnO, we conjecture that local fields may be a major cause of disagreement.

The electronic states computed within the three schemes are used in a calculation of polarization, following the geometric-phase theory reviewed in Ref. 6. The latter has been formulated so far within DFT, and its application within the HF and GW frameworks requires some discussion. At variance with DFT, the HF scheme provides an approximate many-body wave function in the form of a Slater determinant.[11] Let us consider a crystalline insulator with $2N$ electrons per cell and periodic boundary conditions over L cells: the (large) determinant, of size $2LN$, is then built of doubly occupied Bloch orbitals $\psi_n(\mathbf{k},\mathbf{r}) = e^{i\mathbf{k}\cdot\mathbf{r}}\chi_n(\mathbf{k},\mathbf{r})$, where the χ's are lattice-periodical functions, n runs over the N occupied bands, and the Bloch vector $\mathbf{k}$ runs over L allowed values. We may think of this many-body wave function as of the antisymmetrized product of L small determinants, of size $2N$ each, which are built of the occupied spin orbitals at a given $\mathbf{k}$. These small determinants are the basic ingredients defining the geometric phase we are interested in. We start removing the Bloch phase from them, thus defining the $\mathbf{k}$-dependent, lattice-periodical detrimental functions,

$$|\Phi(\mathbf{k})\rangle = |\chi_1(\mathbf{k})\bar{\chi}_1(\mathbf{k})\cdots\chi_N(\mathbf{k})\bar{\chi}_N(\mathbf{k})|. \qquad (1)$$

In the continuum limit ($L\to\infty$), we define the infinitesimal phase difference $d\varphi$ amongst them (alias the Berry connection) in the same way as for one-electron orbitals:

$$d\varphi = -i\langle\Phi(\mathbf{k})|\nabla_{\mathbf{k}}\Phi(\mathbf{k})\rangle\cdot d\mathbf{k}. \qquad (2)$$

Finally, the geometric phase γ yielding the macroscopic polarization can be written as a suitable line integral of Eq. (2): it is easy to prove the equivalence to the alternative forms of $d\varphi$ given in Ref. 6.

We now discuss the application to the model GW case. Being a many-body Green-function scheme, it underlies in principle a correlated ground-state wave function that is not explicitly accessible, while the one-body reduced density matrix *is* accessible, and has a simple expression in terms of the Feynman-Dyson amplitudes. Within the model GW adopted in this work—as in most of the approximate GW schemes for solids—one neglects typically the nonorthonormality of Feynman-Dyson amplitudes. Whenever such an approximation is made, the one-body density matrix is a projector, as for the HF and DFT cases.[12] This basic feature allows the use of the same formulation and implementation of the geometric phase approach in the three cases (HF,

TABLE I. Energies of some one-electron states, relative to the valence-band edge, as computed with the three schemes discussed in the text. The experimental data, from Ref. 3, are also given for comparison.

	HF	Model GW	LDA	Expt.
Γ_{3v} (O $2p$)	−5.7	−5.0	−4.4	−5.2, −5.4
Zn $3d$ (average)	−11.4	−6.4	−5.4	−8.6, −7.5
Γ_{1v} (O $2s$)	−23.4	−18.6	−17.6	−21.0
E_g	11.59	4.23	0.93	3.44

TABLE II. Decomposition of the Born dynamical charges of ZnO into contributions from different groups of bands and from the ionic cores. Notice that within LDA the Zn $3d$ contribution cannot be separated unambiguously from the O $2p$ one. The nominal values, in a completely ionic picture, are also given.

	Atom moved					
	Oxygen			Zinc		
	Nominal	HF	LDA	Nominal	HF	LDA
O $2s$	−2.0	−2.5	−2.4	0.0	+0.5	+0.4
Zn $3d$	0.0	+0.9		−10.0	−10.9	
O $2p$	−6.0	−6.5		0.0	+0.5	
Zn $3d$ + O $2p$	−6.0	−5.6	−5.6	−10.0	−10.4	−10.4
Core	+6.0	+6.0	+6.0	+12.0	+12.0	+12.0
Total	−2.0	−2.1	−2.0	+2.0	+2.1	+2.0

model GW, and DFT). In fact, we are dealing here with *one-body* physical observables (charges and currents): whenever the density matrix is a projector, the one-body properties are *the same as if* the ground state were a single determinant.[13] The various schemes differ in the criterion guiding the choice of this determinant: minimizing total energy (HF); optimizing removal energies and amplitudes (approximate GW); reproducing the ground-state density (exact DFT); and minimizing a given energy functional (DFT-LDA).

Only polarization *differences* between different states of a given material (such as in pyroelectricity, piezoelectricity, and lattice dynamics) have physical meaning. For the purpose of comparing the three theoretical schemes, we *define* the spontaneous polarization as the difference with respect to an unbiased high-symmetry reference state, as explained in Ref. 4. The spontaneous polarization has been evaluated in the three schemes from wave functions computed at the experimental lattice parameters. In units of C/m^2 we get -0.048 (LDA), -0.047 (GW), and -0.046 (HF), to be compared with the indirect estimate -0.07 ± 0.02 obtained from a model based on nonlinear optical data. The three one-electron schemes lead to a concordant description of the phenomenon and to a similar quality of the results: we anticipate that the Z^* values discussed below confirm this feature.

Within our approach, one can unambiguously partition the total polarization as due to different groups of bands only if they are well separated in energy. This band-by-band decomposition will be limited to the HF and LDA schemes. Looking at Fig. 1, it is clear that within HF we can separate the O $2p$ contribution from the Zn $3d$ one, while this is not possible within LDA. Furthermore, in both cases we can consider the separate contribution of the O $2s$ states (not shown in Fig. 1), which are well isolated at lower energy (Table I). The most informative quantity to discuss is the Born dynamical charge, for which we find 2.1 ± 0.05 within HF, and 2.0 ± 0.05 within LDA, to be compared with the experimental value 2.1. All this indicates an apparently rigid-ion-like behavior of this material, with an effective ionic charge equal to the nominal one. As a matter of fact, ZnO has instead a mixed ionic/covalent character, and the ions move in a strongly nonrigid fashion, carrying with themselves, nonetheless, the nominal value of the macroscopic current. Both features are explained through the band-by-band analysis below.

The present understanding of the occurrence of dynamical charges deviating from the nominal value is based on a change of bonding between interacting atoms, induced by the atomic displacements. This change can be simply modeled at the tight-binding level,[14] and has been thoroughly investigated from first principles in ferroelectric perovskites.[5,15] In ZnO the dynamical charge Z^* is essentially identical to the nominal static one: our rationale for this finding in a material with mixed ionic/covalent character is that occupied and empty states do not mix with each other under ionic displacements. Explicit inspection shows that the lowest conduction states in the neighborhood of the fundamental gap have mainly s character (Zn $4s$ and O $3s$). Therefore they are coupled weakly with the highest valence states and the subspace of the occupied electronic states does not vary with ionic displacements.

Less trivial results come from the band-by-band decomposition, since a strong interaction occurs between the *occupied* electronic states. The displacement-induced variation of bonding is responsible for anomalous contributions to the dynamical charges carried by each group of electronic states. Our complete results are displayed in Table II, where the electronic contributions from the different groups of bands are explicitly shown both for O and Zn, although they are

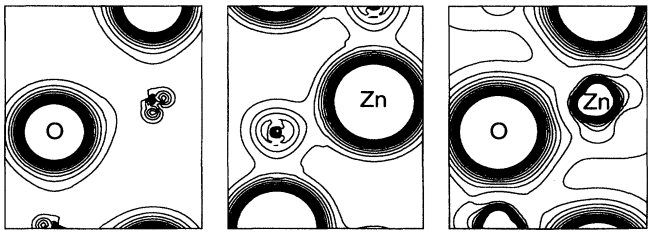

FIG. 2. Decomposition of the Hartree-Fock ground-state electronic density into the contributions from (a) O $2s$ bands, (b) Zn $3d$ bands, and (c) O $2p$ bands. The densities are represented in a plane parallel to the c axis and passing through anions and cations. Subsequent contours differ by 6.25×10^{-3} $e/(\text{a.u.})^3$.

clearly not independent. For the sake of clarity, we also report the positive core charges, and the ideal electronic values (nominal values) corresponding to rigid ions, in a completely ionic picture. The anomalous contributions are immediately identified by comparing nominal and actual values: it is seen that such anomalous contributions are in modulus of the order of 0.5 for O $2s$ and O $2p$, and 0.9 for Zn $3d$. There is practically no difference amongst HF and LDA, wherever the comparison is possible. The biggest surprise is the anomalous contribution of O $2s$ states: since they are very deep in energy (Table I), one would expect them to behave as rigid-core-like states. Instead, the O $2s$ electrons move in a highly nonrigid fashion, due to their non-negligible bonding with Zn $3d$ states, shown in Fig. 2 (a). A similar behavior of O $2s$ states has been recently found in barium titanate.[15] Looking more closely at Table II, one can identify an important qualitative trend. When a given ion is displaced, the electronic states "attached" to this ion carry more (negative) charge than the nominal value (in a totally ionic picture). For instance, analyzing the HF data, an oxygen displacement carries 2.5 effective $2s$ electrons and 6.5 effective $2p$ electrons; analogously, a zinc displacement carries 10.9 effective $3d$ electrons. A similar qualitative trend was previously found in ferroelectric perovskites;[6,5] we conjecture this to be a universal feature of mixed ionic/covalent bonding.

These features are confirmed by the analysis in groups of bands of the ground-state electron charge density at equilibrium. This analysis is most informative at the HF level, where the three relevant groups of bands can be separated unambiguously. We display in Fig. 2 the partial electron densities, which show important deviations from sphericity, a fingerprint of covalence. The charge density of the O $2s$ bands, panel (a), shows a non-negligible bonding with the Zn d orbitals. There are 0.1 and 1.6 electrons in Zn and O spheres, respectively ($R_{Zn}=R_O=1.8$ a.u.). The Zn $3d$ bands, panel (b), are the most perspicuous in accumulating charge in the bonding region (9.0 and 0.3 electrons in Zn and O spheres, respectively): this correlates well with the fact that these same states give the highest anomalous contribution (0.9) to the Born effective charge. The O $2p$ bands, panel (c), display the highest interstitial contribution, since only 0.6 and 3.9 electrons occupy the respective spheres.

Finally, we emphasize that the HF and the LDA approaches provide in ZnO similar and accurate values of the polarization and dynamical charges. The robustness of the calculated properties, and their scheme independence, might appear surprising, given the delicate covalence mechanisms dominating polarization phenomena in mixed ionic/covalent materials. We understand the present findings as a consequence of the fact that interatomic interactions in ZnO occur mostly amongst occupied atomic orbitals from closed shells (O $2s$, O $2p$, and Zn $3d$), and do not involve, practically, the lowest empty ones. As this work, to the best of our knowledge, is the first study comparing the HF, LDA, and model-GW schemes in the framework of polarization, the issue as to whether the scheme-independence holds as well in other materials remains an open one.

We thank A. Dal Corso for his interest in this work and for helpful discussions. This work was supported by the Swiss National Science Foundation (Grant No. 20-39.528.93). Calculations have been performed on the computers of EPF-Lausanne, ETH-Zürich, and ETH-CSCS (Centro Svizzero di Calcolo Scientifico).

[1] See, for instance, C. Campbell, *Surface Acoustic Wave Devices and Their Signal Processing Applications* (Academic Press, San Diego, 1989); I. B. Kobiakov, Solid State Commun. **35**, 305 (1979), and references therein.

[2] P. Schröer, P. Krüger, and J. Pollman, Phys. Rev. B **47**, 6971 (1993).

[3] J. E. Jaffe and A. C. Hess, Phys. Rev. B **48**, 7903 (1993).

[4] A. Dal Corso, M. Posternak, R. Resta, and A. Baldereschi, Phys. Rev. B **50**, 10 715 (1994).

[5] M. Posternak, R. Resta, and A. Baldereschi, Phys. Rev. B **50**, 8911 (1994).

[6] See R. Resta, Rev. Mod. Phys. **66**, 809 (1994), and references therein.

[7] F. Gygi and A. Baldereschi, Phys. Rev. Lett. **62**, 2160 (1989).

[8] S. Massidda, A Continenza, M. Posternak, and A. Baldereschi, Phys. Rev. Lett. **74**, 2323 (1995).

[9] H. J. F. Jansen and A. J. Freeman, Phys. Rev. B **30**, 561 (1984).

[10] S. Massidda, M. Posternak, and A. Baldereschi, Phys. Rev. B **48**, 5058 (1993).

[11] C. Pisani, R. Dovesi, and C. Roetti, *Hartree-Fock Ab-Initio Treatment of Crystalline Systems* (Springer, Berlin, 1988).

[12] Within DFT, the projector over the Kohn-Sham occupied orbitals is the density matrix of the fictitious noninteracting system, *not* of the interacting one. However, since both share by construction the same density, the following considerations remain correct.

[13] Needless to say, matters are completely different whenever two-body properties, such as the total energy, are concerned.

[14] W. A. Harrison, *Electronic Structure and the Properties of Solids* (Freeman, San Francisco, 1980).

[15] Ph. Ghosez, X. Gonze, Ph. Lambin and J.-P. Michenaud, Phys. Rev. B **51**, 6765 (1995).